Article

Spatio-temporal Patterns of Net Primary Production(NPP) in Weihe Watershed(China) and its Response to Environmental Factors

Lixia Wang [1,*], Mingshuang Zhang [2], Zhao Liu [3], Shuangcheng Zhang [1], Jinling Kong [1]

[1] School of Geological Engineering and Geomatics, Chang'an University, Xi'an 710054, China; zylxwang@chd.edu.cn (L.W.); shuangcheng369@chd.edu.cn (S.Z.); jlkong@163.com (J.K.)
[2] School of Earth Sciences and Resources, Chang'an University, Xi'an 710054, China; 2018127009@chd.edu.cn
[3] School of Environmental Science and Engineering, Chang'an University, Xi'an 710054, China; lz975@chd.edu.cn (Z.L.)
* Correspondence: zylxwang@chd.edu.cn

Received: date; Accepted: date; Published: date

Abstract: Spatial and temporal variation characteristics of the net primary production (NPP) and its response to environmental factors are crucial in studying global climate change and terrestrial ecosystem carbon cycles. In this study, Carnegie-Ames-Stanford Approach (CASA) and CA-Markov models are coupled to simulate and predict NPP in the Weihe Watershed using multi-source datasets to explore the spatial and temporal distribution of NPP and its dynamic changes. Correlation analysis was used to quantitatively evaluate the NPP response to environmental factors such as temperature, precipitation, altitude, slope, and aspect. Results showed that: (1) Seasonal and periodic changes were evident within a year, among which the NPP in July was the highest at 115.29 gC/m^2a and the NPP in January the lowest at approximately 10.75 gC/m^2a. The interannual change showed a rising trend. According to forecast results, the NPP status of vegetation in the Weihe Watershed will improve and continue to grow over the next decade. (2) Spatially, the NPP distribution is significantly different. The NPP values in the upper reaches of the Beiluohe and Jinghe Rivers, Baojixia of the Weihe River, and some areas of the Guanzhong Plain are relatively low. The NPP values in the middle and lower reaches of the Beiluohe and Jinghe Rivers and of the Qinling Mountains are relatively high, showing an overall high distribution in the south and east and low distribution in the north and west. (3) The response of vegetation NPP in the Weihe Watershed to environmental factors is significant but varied. The NPP response to temperature and precipitation was mildly positively correlated. The NPP showed trends of stabilizing, then sharply decreasing, and finally increasing with the increase in altitude, as well as continuously increasing with the increase in slope. Meanwhile, the vegetation NPP values of the northern and western slopes were higher than those of the southern and eastern slopes. (4) The CASA and CA-Markov models have high coupling degrees, reaching a prediction accuracy of 0.8776, which is suitable for the simulation and prediction of NPP in the Weihe Watershed. This study is of great significance for understanding the carbon cycle characteristics of regional terrestrial ecosystems, rational utilization of vegetation resources, evaluation of the benefits of ecological construction projects, and formulation of watershed ecological construction and sustainable development strategies.

Keywords: net primary productivity (NPP); simulation; prediction; environmental factor response; predictive model; Weihe Watershed

1. Introduction

At the 19th National Congress of the Communist Party of China (CPC), General Secretary Xi Jinping pointed out that China should "treat the ecological environment like life." Under the guidance of this policy, we will move towards a new era of ecological vegetation civilization. The net primary productivity (NPP) of vegetation is the net increase in organic matter produced by land plants per unit time and unit area by photosynthesis [1]. It reflects the efficiency of plant transformation and the fixation of photosynthetic products and the productivity of plant communities under natural environmental conditions [2]. It is also the study basis of the movement of matter and energy in terrestrial ecosystems, which represents important variables of vegetation activities and the main factors that regulate ecological processes. Moreover, it plays an important role in the analysis of climate change [3].

Since the 1970s, the research on vegetation NPP has gained increasing attention. Many relevant calculation models have emerged, including statistical, process, and parameter models [4–9]. NPP estimation models extend site data to regional and even global scales; the Carnegie-Ames-Stanford Approach (CASA) model is a typical representative of this model [10–16]. In particular, after the optimization of this model by Zhu et al. in 2007, its applicability was improved and it could be used to develop estimates at different scales and regions [17].

Relevant scholars at home and abroad have carried out a lot of research on the spatio-temporal dynamic change and driving factors of NPP and other scientific issues, and have also achieved fruitful results [18–20]. Nemani et al., for example, studied the development of the global climate and concluded that it is conducive to the growth of vegetation [15]. Bokhorst et al. estimated the vegetation restoration after extreme winter warming events in subarctic regions. Neumann et al. compared the net primary productivity of Moderate Resolution Imaging Spectroradiometer (MODIS) vegetation with the inventory data of Austria's terrestrial national forest [21]. Zhu et al. systematically analyzed the NPP and corresponding climatic data of China's terrestrial vegetation from 1982 to 1999 [17]. Chen et al. estimated the relationship between NPP and climatic factors in different periods [22]. At the same time, the spatio-temporal characteristics of vegetation NPP in different regions of China, such as the Qinghai-Tibet Plateau, Loess Plateau, northeast China, southeast China, and subtropical hilly areas, and their response to climate change have also been widely studied. These studies are of great significance in revealing the spatial and temporal pattern characteristics, changing processes, and driving mechanisms of NPP in terrestrial ecosystems [23–28]. Remote sensing data provide important information about the dynamic change process of vegetation type/vegetation cover. The use of remote sensing data to predict the dynamic change of vegetation can obtain the growth status of vegetation in the future to carry out disaster risk estimations and crop yield predictions. Many scholars at home and abroad have conducted extensive and in-depth exploration and established relevant prediction models [29–33]. For example, Funkc et al. used the lag relationship between the normalized difference vegetation index (NDVI) and precipitation to establish an empirical model to predict NDVI changes in semi-arid regions in Africa [34]. Goncalves et al. used multivariable and univariate models to predict the crop NDVI in the Sao Paulo sugarcane producing area in Brazil [35].

The study of the characteristics, changes, and distribution of the natural geographical environment and its components is usually based on the law of natural geographical differentiation [36]. However, a review of many domestic and foreign studies on the temporal and spatial distribution and variation

characteristics of regional vegetation NPP has shown that there are relatively abundant simulation studies at the administrative region scale, while few prediction studies have been conducted at watershed scales. There are many studies on the response of vegetation NPP to climate factors such as temperature and precipitation but few studies on its response to topographic factors. There have been many studies on vegetation NDVI prediction, but few studies on vegetation NPP prediction [37,38]. Therefore, it is of great theoretical significance to simulate and predict the spatial and temporal distribution characteristics of watershed-scale vegetation NPP and explore its correlation with environmental factors. At the same time, the Weihe Watershed is one of the most important regions in the northwest of China. It is facing severe ecological deterioration, which has mainly manifested as serious economic water diversion, frequent river discontinuities, and excessive groundwater exploitation [39,40].

This study takes the Weihe Watershed as the research object, based on the CASA model, correlation analysis, and CA-Markov model using MODIS NDVI data and meteorological data, vegetation type data, and DEM data; comprehensively considers the time of cultural factors, such as the Returning Farmland to Forest Program and Hanjiang to Weihe River Project; selects 2000, 2006, 2012, and 2018 as research periods; estimates the spatial and temporal distribution characteristics and dynamic change rules of NPP vegetation in the Weihe Watershed; makes a quantitative analysis of its response degree precipitation, temperature, altitude, slope, and aspect; and predicts the spatial distribution pattern of NPP in the Weihe Watershed in 2024 and 2030. The rest of this paper is structured as follows: Section 2 introduces the research area and data processing, Section 3 introduces the research methods, Section 4 analyzes the research results, the discussion is provided in Section 5, and Section 6 presents the conclusions of this study.

2. Data sources

2.1. Study area

The Weihe River is the largest tributary of the Yellow River. It originates from the Niaoshu Mountains in Weiyuan county, Dingxi, Gansu province; flows through three provinces (regions) of Gansu, Ningxia, and Shaanxi; and flows into the Yellow River in Tongguan County, Weinan, Shaanxi province, with a total length of 818 km and a total basin area of 134,800 km^2, located between 33°40′ – 37°18′ N and 106°20′ – 110°37′ E, as shown in Figure 1 [31]. To the south of Weihe River lie the Qinling Mountains; to the north lies the Liupanshan Mountain. The watershed can be divided into two parts: the western part is the Loess Hilly and Gully region and the eastern part is the Guanzhong plain region. The watershed is located in the arid and semi-arid region of northwest China, with a continental monsoon climate. The winter is cold and dry and precipitation is rare, while the summer is hot and rainy. The annual average temperature is 7.8–13.5 °C and the annual average precipitation is 500–800 mm [32]. The Weihe Watershed is an important agricultural, industrial, and energy base in China and the core hub of northwest China. In recent years, with the rapid development of society and economy, the ecological environment problems in the Weihe Watershed have become more and more severe, attracting more and more attention from all sectors of society [29].

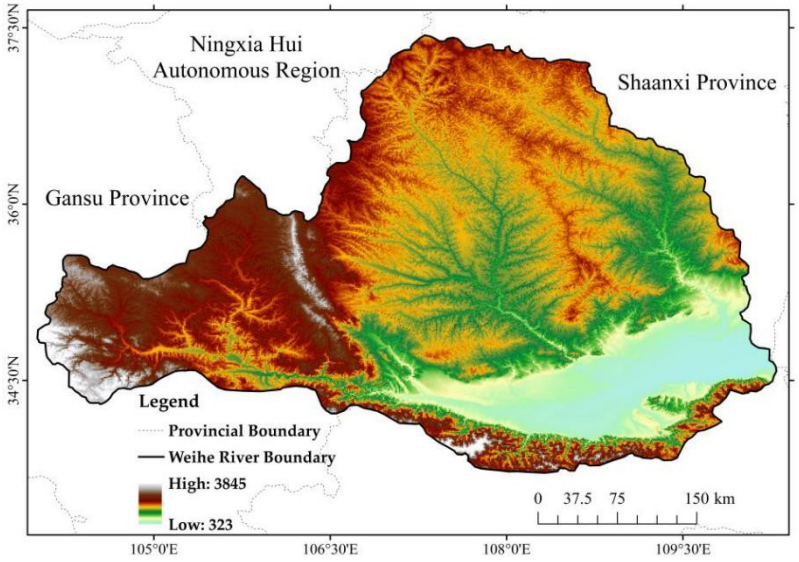

Figure 1. Geographical location and topography of the Weihe Watershed.

2.2. Data sources

1. Remote sensing data (mainly NDVI data): The data selected in this study are MOD13Q1 data from the NASA website (https://ladsweb.modaps.eosdis.nasa.gov/). The spatial resolution was 250 m. To facilitate the reading and processing of ENVI and ArcGIS software as well as the spatial matching of the existing map data, preprocessing such as splicing, projection conversion, and format conversion is required. Therefore, Modis Reprojection Tools (MRT) were used for preprocessing. At the same time, the image data is affected by the atmosphere, soil, height angle, and other factors, resulting in noise in the NDVI value. Therefore, the maximum value synthesis method is selected to synthesize the two phases of NDVI data every month.

2. Meteorological data (including sunshine hours, temperature, and precipitation): The data used in this study were obtained from the National Meteorological Information Center (http://data.cma.cn/), including 33 meteorological stations in and around the Weihe Watershed. As there are few stations observing radiation data nationwide, the radiation derivation formula is used to convert sunshine hours into radiation data. Finally, sunshine radiation, average daily temperature, and average daily precipitation data were interpolated into raster data with spatial resolution consistent with NDVI using the Kriging interpolation method.

3. Other data: Digital elevation model (DEM) data, administrative boundary data, vegetation type data, etc., were derived from the geospatial data cloud (http://www.gscloud.cn/). DEM data were spliced and clipped in ArcGIS to obtain DEM data covering the study area. Then, the spatial resolution was resampled to 250 m and slope and aspect information was extracted for overlay analysis with NPP data.

3. Method

3.1. CASA model

The CASA model is a parametric model based on the light energy utilization principle developed by Potter and Field according to Monteith's theory of calculating NPP using photosynthetically active radiation (APAR) and efficiency for solar energy utilization (ε) [9,41–43]. The model has been widely used in large-

scale vegetation NPP simulations and global vegetation carbon cycles, and has been calibrated by more than 1,900 field sites worldwide [44]. In this study, the improved CASA model of Zhu Wenquan was used to estimate the vegetation NPP of terrestrial ecosystems in the Weihe Watershed in 2000, 2006, 2012, and 2018.

According to the physiological and ecological processes, the model-simulated NPP of vegetation is mainly determined by the photosynthetically active radiation absorbed by vegetation and efficiency of solar energy utilization [45]. The calculation formula is as follows:

$$NPP(x,t) = APAR(x,t)(x,t), \quad (1)$$

where t is the time and X is the position in space.

3.2. Correlation analysis

Correlation analysis is an effective method to reveal the degree of correlation between variables [29]. This study analyzes the correlation between NPP, climatic factors, and topographic factors based on a pixel scale; discusses their response degree; and analyzes their spatial distribution. The formula for calculating the coefficient of association is

$$R_{xy} = \frac{\sum_{i=1}^{n}(x_i - x)(y_i - y)}{\sqrt{\sum_{i=1}^{n}(x_i - x)^2 (y_i - y)'}} \quad (2)$$

where R_{xy} is the correlation coefficient; x_i and y_i represent the values of variables x and y, respectively, in period i; x and y are the average values of variables x and y, respectively; and n is the sample size. The value range of the correlation coefficient is -1–1, positive values represent the positive correlation between variables, and negative values represent the negative correlation between variables. The greater the absolute value of the correlation coefficient, the stronger the correlation between variables.

A significance test of the calculated correlation coefficients was carried out using the phase lookup relation table. Taking the significance level as $\alpha = 0.05$ and $\alpha = 0.01$, the table was checked and values of $f\alpha(n-2) = f0.05(2) = 0.811$ and $f\alpha(n-2) = f0.01(2) = 0.917$ were obtained. The correlation coefficients can be divided into six levels according to their significance: Significantly negative correlation ($R < -0.917$), moderately negative correlation ($-0.917 < R < -0.811$), mildly negative correlation ($-0.811 < R < 0$), mildly positive correlation ($0 < R < 0.811$), moderately positive correlation ($0.811 < R < 0.917$), and significantly positive correlation ($R > 0.917$).

3.3. CA-Markov model

Cellular automata is a local grid dynamic model with discrete time, space, and state [46]. This method has a powerful ability to simulate the spatio-temporal evolution of complex systems and is widely used in the research of land change, population migration, urbanization, and other fields. The standard cellular automata is a quaternion composed of cellular, state, neighborhood, and rules, which is expressed as follows:

$$A = (d, s, n, f), \quad (3)$$

where A represents the cellular automata system, d is the positive integer representing the dimension of the cell, s represents the state set of the cell, n is the

neighborhood of the cell, and f represents the transformation rule of the cellular state in the local space. Thus, the cellular automata model can be expressed as:

$$S_{ij}^{t+1} = f_n(S_{ij}^t), \quad (4)$$

where S represents the state of the cell, f is the transition function, and the transition rule of the cell from time t to time t+1 is defined. N is the neighborhood of the cell and belongs to an input variable f. Cellular evolution in a local space can be realized by applying the defined transformation rules.

The Markov model is a special random motion process with no aftereffect, which has been applied in the simulation and prediction of many geographical phenomena [47]. In recent years, the Markov model has been gradually applied to vegetation ecological prediction and landscape change research.

The basic principle of the Markov model is to use the empirical transfer probability between the discrete states in the observation system to determine the change trend of each state in the system, to predict future states [48]. In this study, the NPP state of a single-pixel scale is regarded as a random process and the level of NPP value of the pixel is regarded as the state of the Markov chain. In the Markov model, the change in the NPP state is random.

Both the CA model and Markov model are time-discrete and state-discrete dynamic models; however, the Markov model cannot predict the spatial variables of vegetation change. Moreover, the CA model has a strong ability to simulate the spatio-temporal evolution of complex spatial systems [49]. The CA_Markov module in IDRISI17.0 software combines the two to simulate the spatial and temporal patterns of vegetation change.

4. Results

4.1. Temporal variation characteristics of the NPP

In this study, the monthly (Figure 2), seasonal (Figure 3), and annual (Figure 4) vegetation NPP variation in the Weihe Watershed in 2000, 2006, 2012, and 2018 were calculated; the monthly(Figure 5), seasonal (Figure 6), and annual (Figure 7) vegetation NPP variation trends were also plotted.

From a monthly-scale perspective, the variation curve shows a unimodal pattern during the year and the time distribution of NPP in the year is characterized by a gradual increase from January to July, followed by a gradual decrease from August to December. The monthly mean of the highest vegetation NPP appeared in July at approximately 115.29 gC/m^{2}a, and the monthly mean of the lowest vegetation NPP appeared in January at approximately 10.75 gC/m^{2}a.

From the perspective of seasonal scale, the seasonal and periodic variation of vegetation NPP in the Weihe Watershed was evident. The seasonal variation of the vegetation NPP during the year directly reflects the phenology of vegetation. In summer, the vegetation is in the vigorous growth stage, and the vegetation NPP is the highest at approximately 382.08 gC/m^{2}a. In spring, the temperature increases, precipitation increases, and the growth rate of vegetation accelerates. Therefore, the vegetation NPP is second only to that of summer at approximately 129.38 gC/m^{2}a. In autumn, the vegetation gradually stops growing until it withers and the vegetation coverage gradually decreases. Therefore, the NPP of the vegetation gradually decreases, at a rate slightly lower than that of spring, which is approximately 118.94 gC/m^{2}a. The vegetation NPP in winter was the lowest, at approximately 42.97 gC/m^{2}a.

From an annual perspective, the annual vegetation NPP in the Weihe

Watershed generally presents an upward trend. Between 2000 and 2006, the annual average vegetation NPP values were approximately 549.12 gC/m^{2}a and 700.88 gC/m^{2}a, respectively. The annual mean vegetation NPP in 2012 was essentially the same as that in 2006, at approximately 770.85 gC/m^{2}a. The annual mean vegetation NPP in 2018 increased slightly to approximately 828.00 gC/m^{2}a.

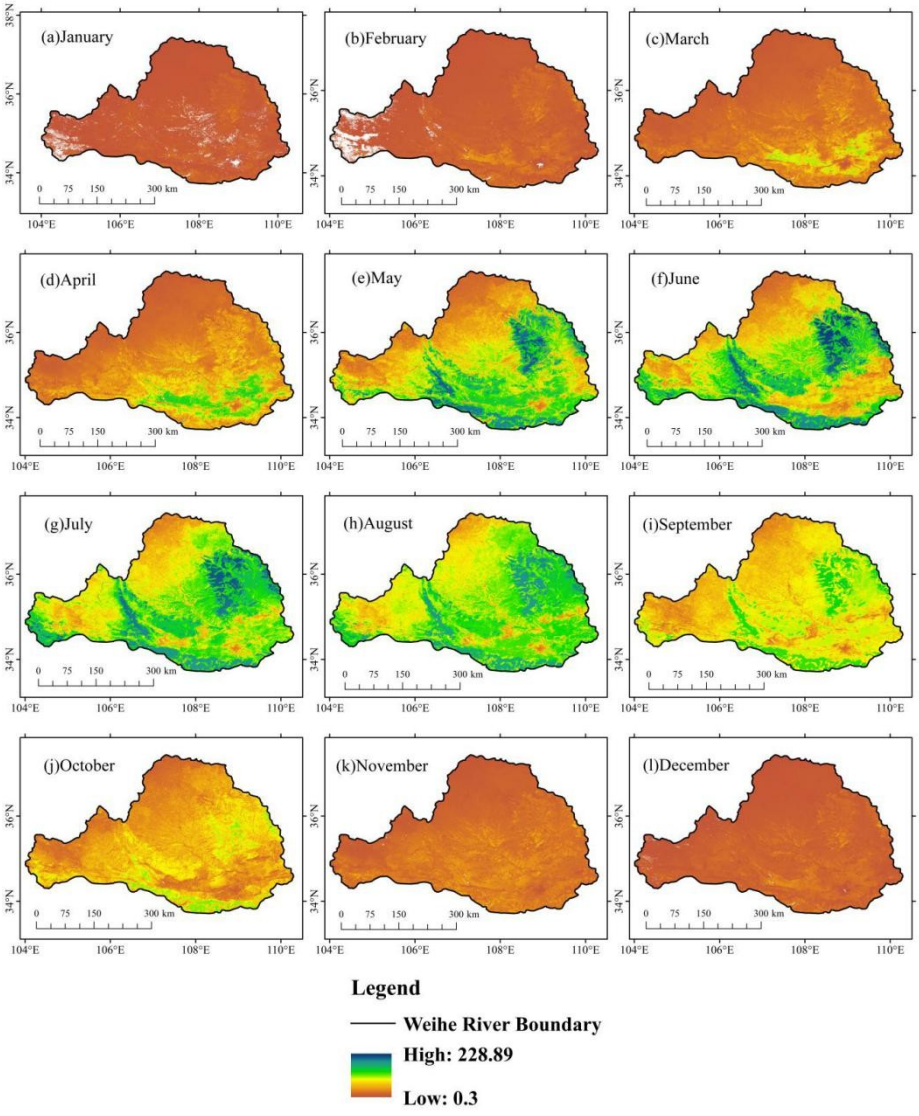

Figure 2. Spatial distribution of NPP in each month in the Weihe Watershed.

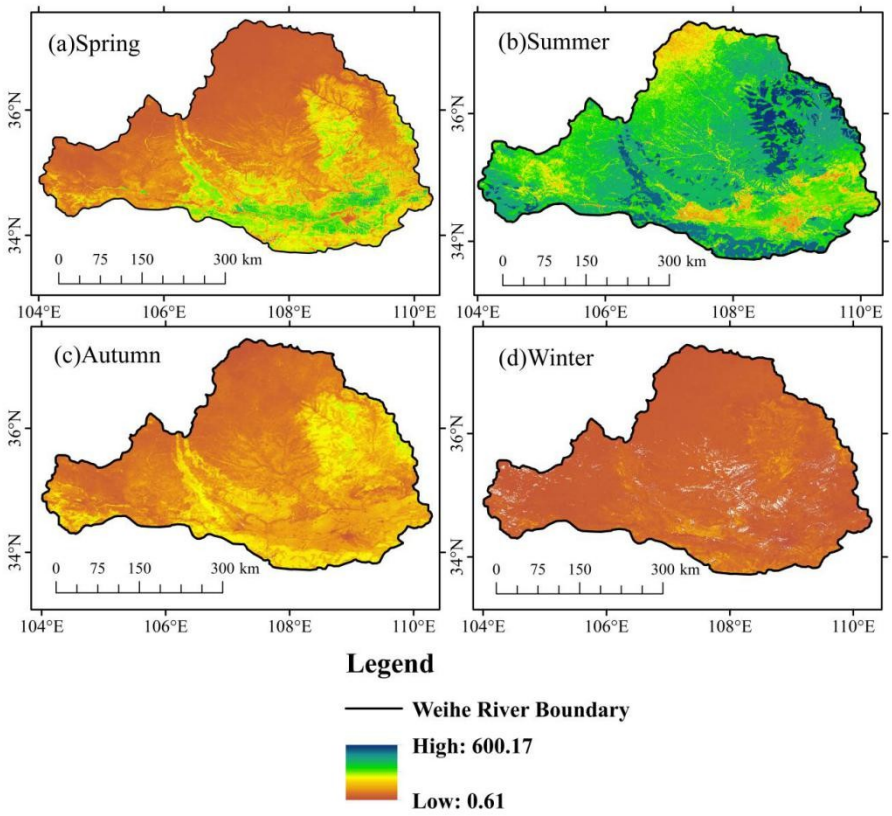

Figure 3. Spatial distribution of NPP in different seasons in the Weihe Watershed.

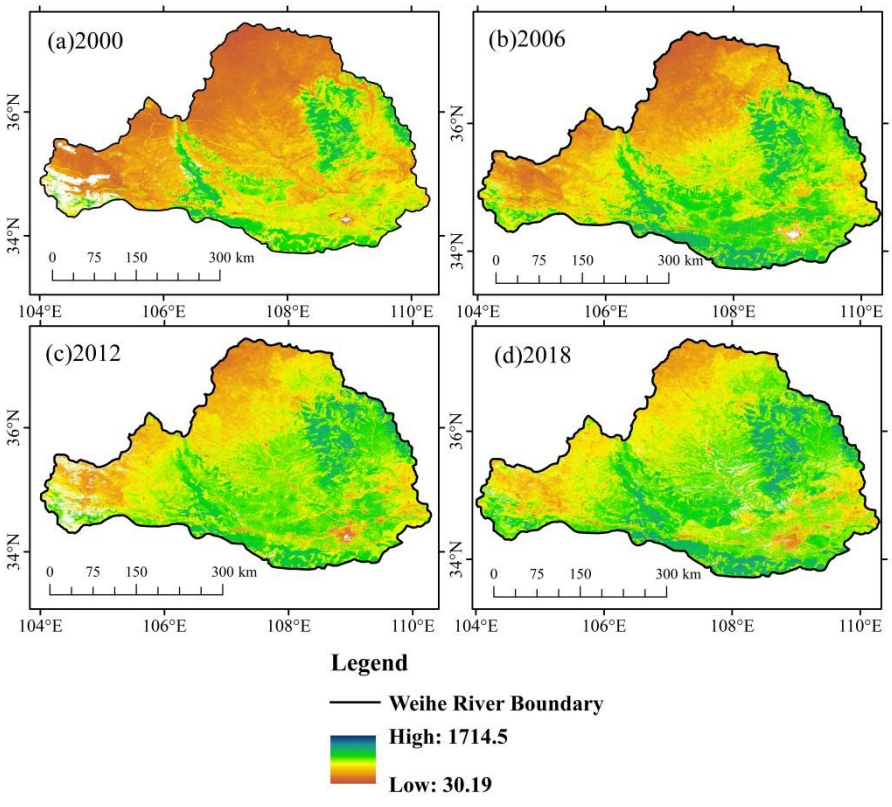

Figure 4. Spatial distribution of NPP in 2000, 2006, 2012, and 2018 in the Weihe Watershed.

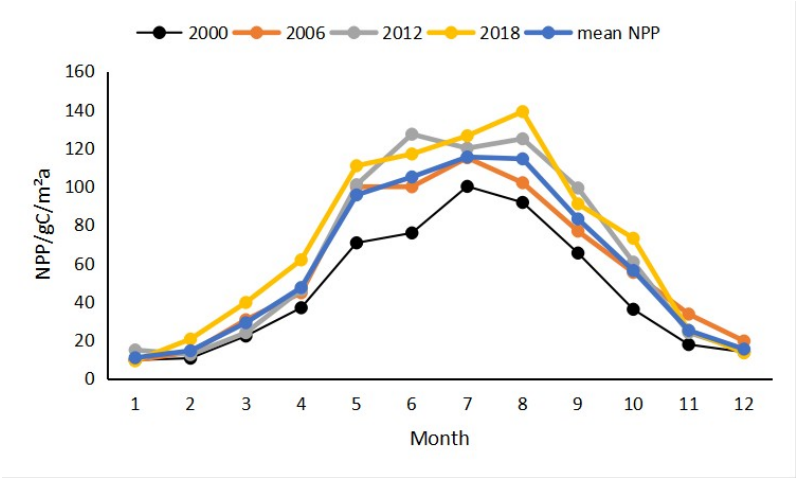

Figure 5. NPP change trend in each month in the Weihe Watershed.

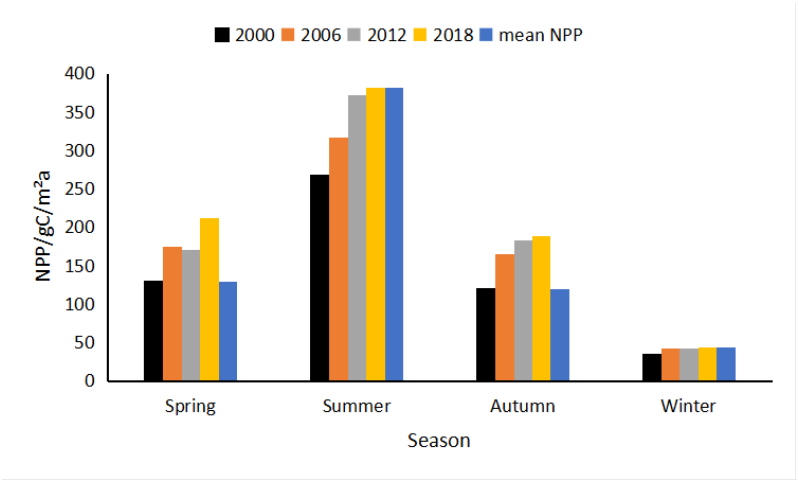

Figure 6. NPP change trend in different seasons in the Weihe Watershed.

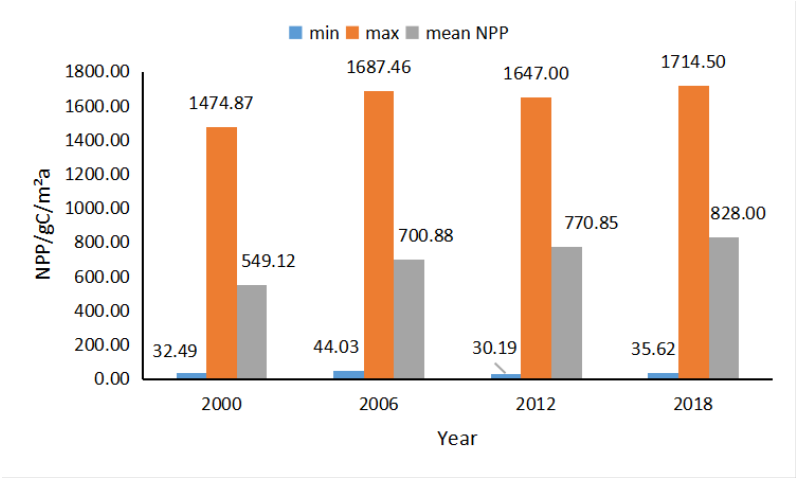

Figure 7. NPP change trend in 2000, 2006, 2012, and 2018 in the Weihe Watershed.

4.2. Spatial distribution characteristics of the NPP

Through simulation, the annual mean NPP in the Weihe Watershed in 2000, 2006, 2012, and 2018 was obtained, mainly concentrated between 114.14 and 1557.80 gC/m²a, with an average of approximately 715.08 gC/m²a. The spatial distribution characteristics of vegetation NPP in each year are similar, showing high distribution characteristics in the south and east and low ones in the

north, and west, with obvious spatial differences, as shown in Figure 4. Among them, the region of the Qinling Mountains has a low latitude and the vegetation is mainly evergreen broad-leaved forest, with abundant annual precipitation and high annual temperature. The vegetation type above the Beiluohe-Zhuangtou region is mostly deciduous broad-leaved forest and the temperatures and precipitation are higher than those in the western region; therefore, the annual average NPP in these areas is higher. The main vegetation types in the Guanzhong Plain, above Zhangjiashan of the Jinghe River and above Baojixia of the Weihe River are cultivated plants. In addition, as the latitude increases gradually, the temperature decreases gradually, the precipitation decreases gradually, and the annual average vegetation NPP also decreases gradually. The average annual NPP of vegetation in the north of the Weihe Watershed is the lowest because the higher the latitude and elevation are, the lower the temperature is, and the lower the precipitation is.

4.3. Response of NPP to major climatic factors

The Weihe watershed is located in the transition zone between the semi-humid and semi-arid regions of China. Due to its geographical location, the difference in topography between north and south, difference in atmospheric circulation conditions, and spatial distribution of temperature and precipitation in the Weihe Watershed varies. In this study, the Kriging interpolation method is used to carry out spatial interpolation on the average temperature and precipitation of the Weihe Watershed and 33 surrounding meteorological stations. The spatial distribution of the average annual temperature and precipitation of the Weihe Watershed was obtained, as shown in Figures 8 and 9.

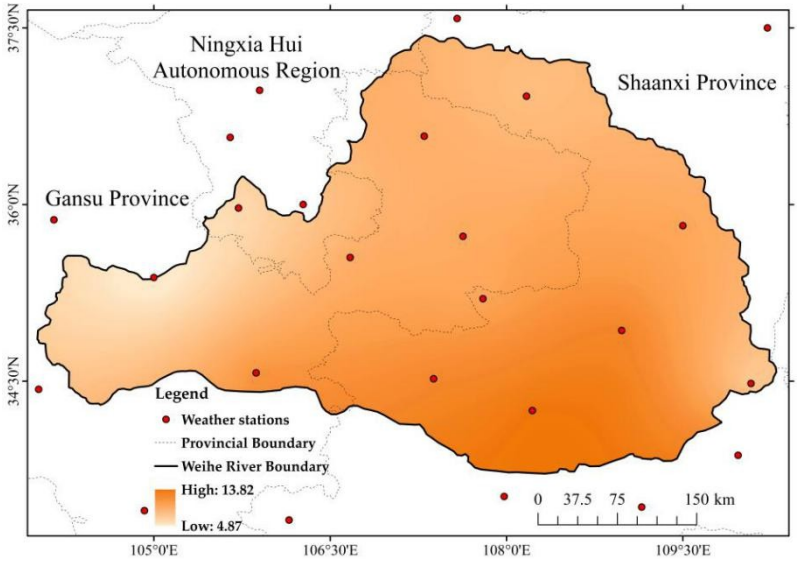

Figure 8. Spatial distribution of annual average temperature in the Weihe Watershed.

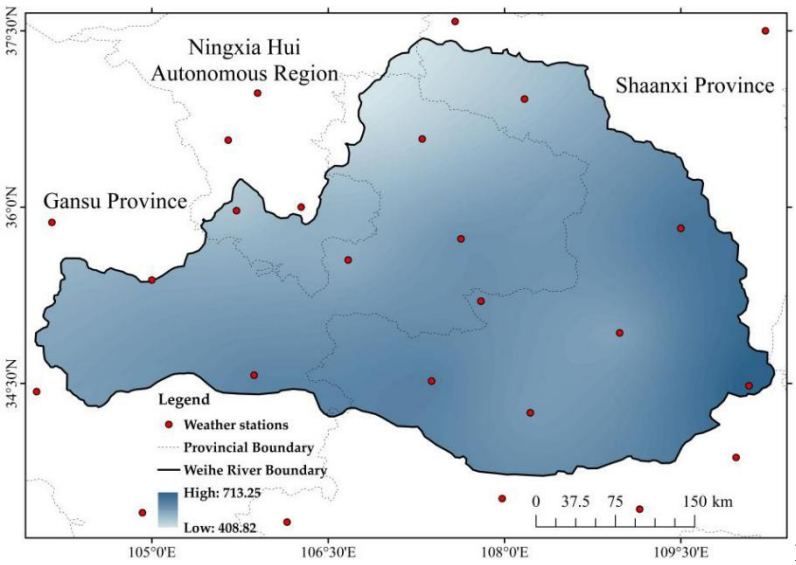

Figure 9. Spatial distribution of annual average precipitation in the Weihe Watershed.

4.3.1. Time variation characteristics of major climatic factors

The temporal variation trend of temperature and precipitation in the Weihe Watershed is highly consistent. Both temperature and precipitation have obvious seasonal changes, with low temperatures and low precipitation in the winter and high temperatures and high precipitation in the summer. The annual mean values of temperature and precipitation in each month were calculated and the time distribution characteristics of temperature and precipitation in the Weihe Watershed were obtained. The highest average temperature was 22.26 °C in July and the lowest was -4.11 °C in January. The maximum average precipitation was 100.53 mm in August and the minimum was 3.65 mm in December. The interannual fluctuation of temperature and precipitation was small and there was no obvious fluctuation period. The highest average temperature was 10.10 °C, and the perennial average precipitation was 569.18 mm. The highest temperature was 10.67 °C in 2006 and the lowest was 9.4 °C in 2012. The greatest precipitation occurred in 2018 at 751.49 mm and the smallest occurred in 2000, at 488.51 mm.

4.3.2. Spatial distribution of major climatic factors

According to the interpolation results, the average temperatures of the Weihe Watershed for several years are between 4.87 °C and 13.82 °C; the spatial distribution features are high in the south and east and low in the north and west. Among them, the temperature in the Guanzhong Plain is relatively high. The farther north in the Guanzhong Plain, the higher the temperature decreases with the gradual increase in latitude and altitude. The main reason for this is that the Guanzhong Plain has low latitude and altitude. The upper reaches of the Weihe River are relatively low in temperature mainly because of the high altitude of the region.

The average annual precipitation of the Weihe Watershed is between 408.82~713.25 mm, gradually decreasing from the southeast to northwest in space. The precipitation from Xianyang of the Weihe River to Tongguan is the most abundant; the farther to the west and north, the more the precipitation gradually decreases. The main reason for this is that the northwest is deep inland, far away from the sea, and the topography of the humid airflow is blocking.

4.3.3. Response of NPP to major climatic factors

Figures 10 and 11 show the general relationship between average monthly vegetation NPP, temperature, and precipitation in the Weihe Watershed. As can be seen from Figure 10, there is a significant linear correlation between the NPP of vegetation and temperature. The vegetation NPP increases with the increase in temperature. When the monthly average temperature is above 20 °C, the NPP of vegetation tends to reach a maximum. The NPP of vegetation also increases with the

increase in precipitation. When the monthly average precipitation exceeded 1000 mm, the vegetation NPP tended to be stable, indicating that the water supply for the growth and development of vegetation tended to be saturated.

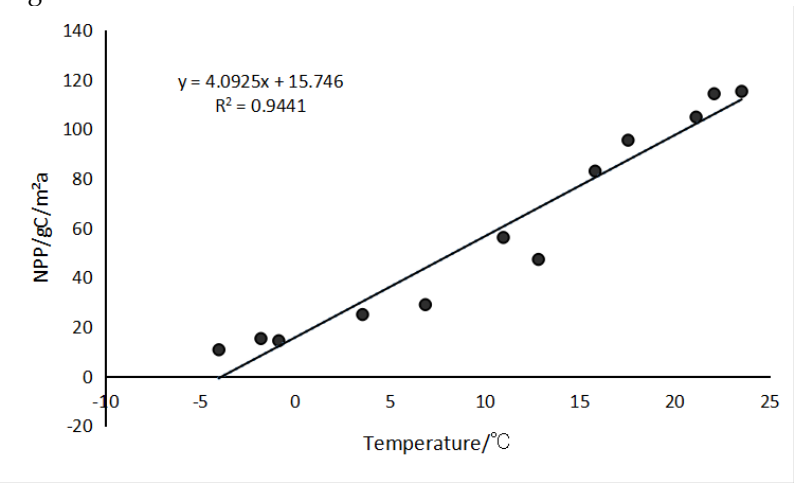

Figure 10. Relationship between NPP and temperature in the Weihe Watershed.

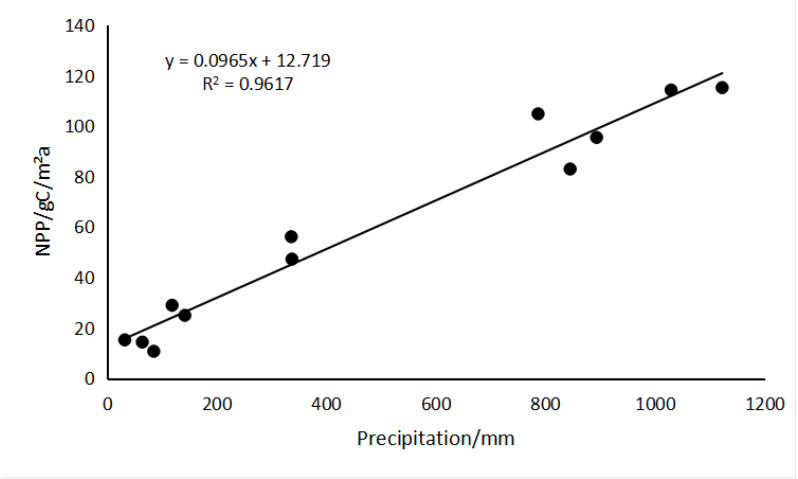

Figure 11. Relationship between NPP and precipitation in the Weihe Watershed.

To further quantitatively analyze the correlation between the vegetation NPP, temperature, and precipitation, their correlation coefficients were calculated as shown in Figure 12 and Table 1. They show the spatial distribution of the correlation coefficient between the vegetation NPP, temperature, and precipitation in the Weihe Watershed as well as the number of pixels and proportion of each correlation level.

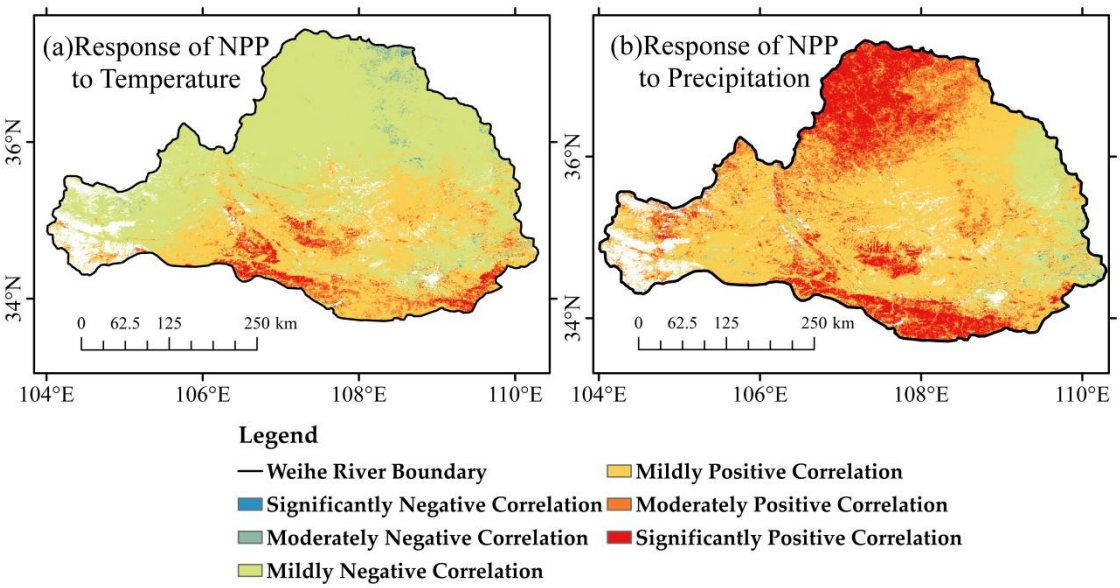

Figure 12. Spatial distribution of correlation between NPP, temperature, and precipitation in the Weihe Watershed.

Table 1. Correlation statistics of NPP and temperature and precipitation in the Weihe Watershed

Correlation Level	Temperature		Precipitation	
	Number of Pixels	Proportion/ %	Number of Pixels	Proportion/ %
Significantly negative correlation	4,697	0.23	3,697	0.18
Moderately negative correlation	2,6342	1.31	6,205	0.31
Mildly negative correlation	116,9454	58.11	221,011	10.98
Mildly positive correlation	656,835	32.64	1129,895	56.14
Moderately positive correlation	89,274	4.44	329,562	16.38
Significantly positive correlation	65,889	3.27	322,120	16.01

According to the calculated results, the correlation coefficient between NPP and temperature is between -0.99 and 0.99. In general, the relationship between NPP and temperature in the Weihe Watershed was mainly mildly positive and mildly negative, with pixel proportions of 32.64% and 58.11%, respectively, which were distributed in the northern part of the study area, the Guanzhong Plain area, and specific portions of the southern part of the study area. The proportion of pixels with a moderately negative correlation and significantly negative correlation between NPP and temperature in the whole region is small (1.54%). The proportion of pixels with moderately positive correlation and significantly positive correlation between NPP and temperature was 7.71%, mainly distributed in the southern Qinling mountains.

The correlation coefficient between NPP and precipitation was between -0.99~1. This shows that NPP is mainly mild, moderate, and significantly positively correlated with precipitation in the Weihe Watershed; it is stronger in the south and north than in the middle, with pixel proportions of 56.14%, 16.38%, and 16.01%, respectively, distributed in the central and western regions and the northern and southern parts of the regions. Pixels with a mildly negative correlation, moderately negative correlation, and significantly negative correlation between NPP and precipitation in the whole region accounted for a small proportion (11.47%), mainly distributed in the eastern region. In general, vegetation NPP in the Weihe Watershed has a higher correlation with precipitation.

4.4. Response of NPP to topographic factors

Terrain plays an important role in the redistribution of surface water and heat resources and is the basis for the formation of regional climate type, soil type, and vegetation type. Factors such as surface relief, slope, and aspect are closely related to vegetation coverage. Based on the DEM data of the Weihe Watershed, slope and aspect factors were extracted from the ArcGIS platform and the terrain factors were divided, calculating the mean value of each terrain factor using the statistical function of partition to analyze the spatial distribution of NPP and the response degree between the changes of NPP and the terrain factors.

4.4.1. Response of NPP to elevation.

Figure 13 shows the variation of vegetation NPP with elevation. The mean vegetation NPP fluctuates significantly with the change in altitude and the difference between the maximum value and minimum values is large. In the area with an elevation of less than 1000 m, namely, the Guanzhong plain area, the corresponding mean NPP fluctuates less, remaining between 750.19 and 768.41 gC/m^{2}a, which accounts for 20.17% of the total number of pixels. In the range of elevation from 1000 to 1500 m, the mean vegetation NPP decreased slightly but the difference was not significant at 761.48 gC/m^{2}a, accounting for the highest percentage of the total number of pixels (43.57%); it was mainly distributed in the Jinghe and Beiluohe Watershed. As the elevation rose to 2000 m, the mean vegetation NPP decreased rapidly and the minimum value of 610.04 gC/m^{2}a appeared. The percentage of the total number of pixels decreased slightly, to 28.89%, which was mainly distributed in the northern, northwestern, and western regions. After that, as the elevation continued to rise, the vegetation NPP gradually increased. In the area above 2500 m, the vegetation NPP reaches a maximum value of 869.87 gC/m^{2}a, which is mainly caused by the high vegetation coverage and mostly deciduous broad-leaved forests distributed in the Qinling Mountains, accounting for only 0.94% of the total pixel percentage.

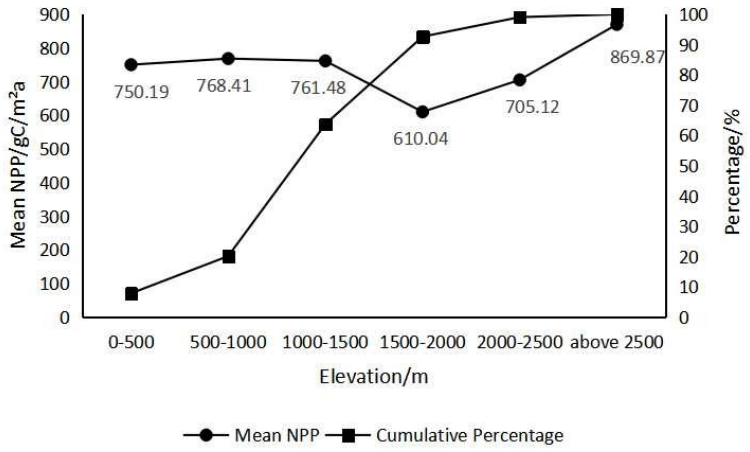

Figure 13. Changes of NPP with elevation in the Weihe Watershed.

4.4.2. Response of NPP to slope

The slope of the Weihe watershed is between 0 ° and 73 °; the slope of more than 90% of the region is less than 30 °. Figures 14 and 15 show the variation of the mean NPP with the increase in slope. In general, with the increase in slope, the average NPP of the vegetation shows an increasing trend. The percentage of the total number of pixels shows an increasing trend of increasing first, which then

decreases. In the slope range of 0–5°, the average vegetation NPP is 678.35 gC/m²a, accounting for 13.95% of the total number of pixels. It is mainly distributed in the plains and river valleys with low elevation. With the continuous increase in slope, the mean NPP of vegetation increases slightly. The percentage of NPP in the total number of pixels increased rapidly. The pixel proportion in the change stage of slope 6–15° was the largest at 37.01%. After that, although the average NPP of vegetation continued to increase with the increase in slope and reached a maximum value of 926.76 gC/m²a in the area above the slope of 46°, the percentage of the total number of pixels in each interval continued to decrease, rapidly decreasing between 26 ° and 40°, with the decrease rate gradually lessened.

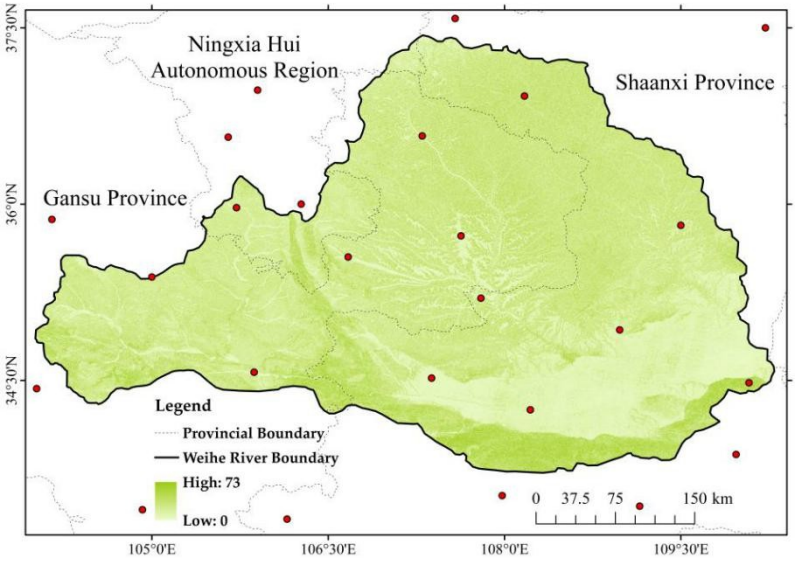

Figure 14. Spatial distribution of slope in the Weihe Watershed.

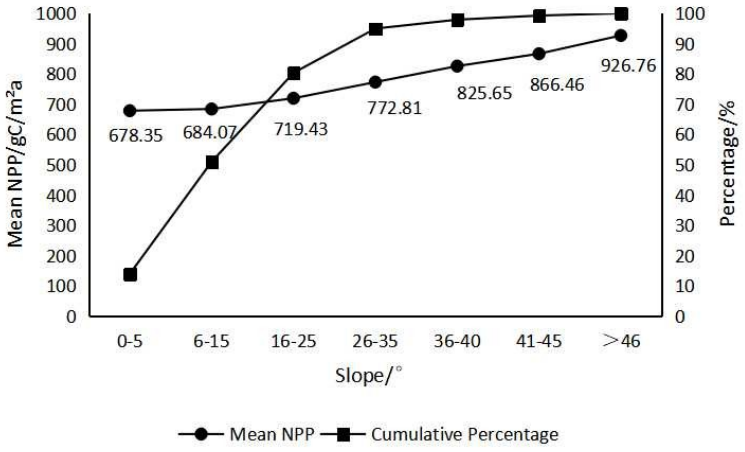

Figure 15. Changes of NPP with slope in the Weihe Watershed.

4.4.3. Response of NPP to aspects

The aspect is defined as the direction of the projection of the slope normal onto the horizontal plane. Different aspects lead to different light, heat, temperature, and other conditions for vegetation growth. By calculating the distribution of aspects in the Weihe Watershed and the mean value of vegetation NPP corresponding to each aspect, the response of vegetation NPP to the change of an aspect can be analyzed [50].

The proportion of each aspect in the Weihe Watershed is flat land (0.49%), north slope (10.93%), northeast slope (12.75%), east slope (13.76%), southeast slope (12.35%), south slope (11.94%), southwest slope (12.40%), west slope (13.18%), and northwest slope (12.20%), as shown in Figure 16. The mean NPP of vegetation corresponding to each aspect is shown in Figure 17. Overall, the mean NPP of vegetation corresponding to each aspect is between 688.3 and 732.34 gC/m^2a. However, there are still some differences between the aspects. The mean NPP of the north slope was higher than that of the south slope; the mean NPP of the west slope was slightly higher than that of the east slope. The mean value of vegetation NPP is as follows from large to small: northwest slope > north slope > northeast slope > west slope > southeast slope > east slope > south slope > southwest slope > flat land.

Differences in hydrothermal conditions can explain this feature. According to the statistics of the average temperature and precipitation in each aspect, the difference in the average annual precipitation in each aspect is approximately 1–3 mm. Meanwhile, the average temperature of the north slope and the west slope is approximately 0.05–0.20 °C lower than that of the southern and eastern slopes. This indicates that in northwest China, the climate is dry and sunny, the north slope is on the dark side, the solar radiation received is relatively less, the evaporation is weak, and the water is easy to retain. Therefore, the northern slope is relatively humid and the respiration of the vegetation is weakened, which is more conducive to the growth of vegetation. There are many results showing that the soil of the north slope and west slope has better water holding capacity, higher soil moisture content, and better vegetation growth than that of the southern and eastern slopes.

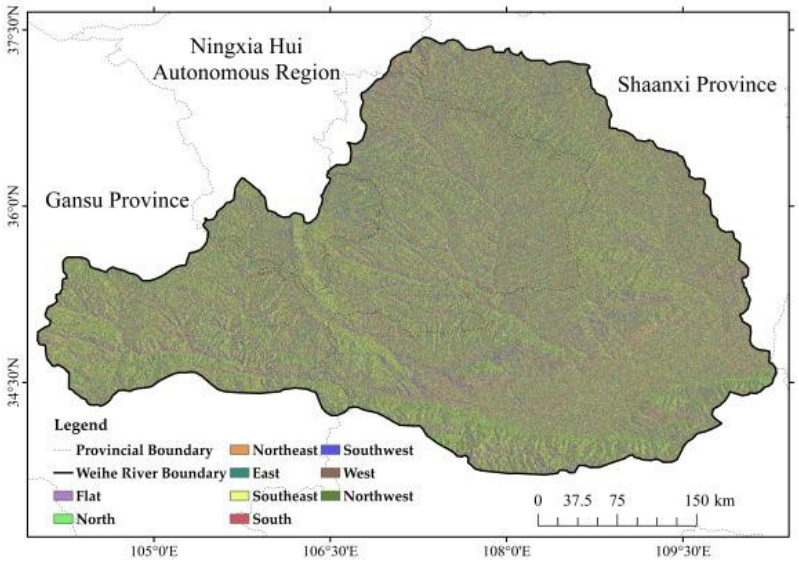

Figure 16. Spatial distribution of aspect in the Weihe Watershed.

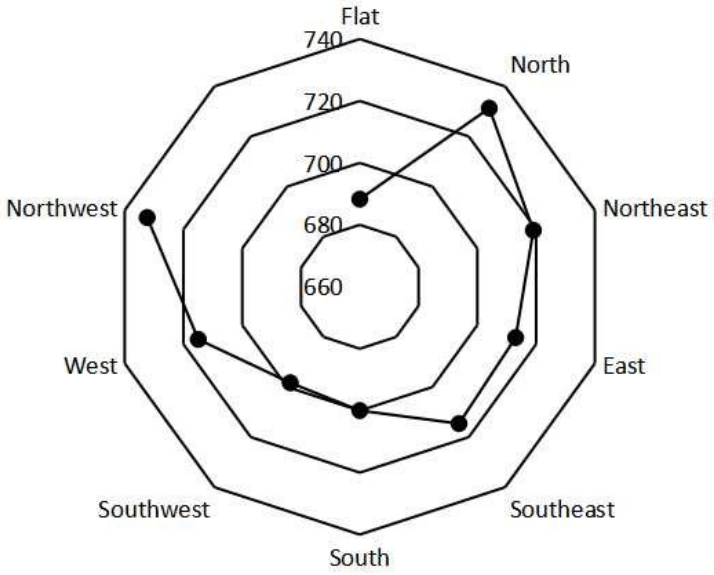

Figure 17. Changes of NPP with aspect in Weihe Watershed.

4.5. Prediction of the NPP spatial distribution pattern

As the input data in the CA-Markov model needs to be spatial and state-discrete raster data, according to the natural discontinuity point classification method, they are divided into five levels: very high-value regions, higher-value regions, medium-value regions, lower-value regions, and very low-value regions. The area and percentage of each NPP grade in 2012 and 2018 were calculated as shown in Table 2. The overall characteristics of the NPP status in the Weihe Watershed in 2012 mainly correspond to lower-value regions, medium-value regions, and higher-value regions, which account for 75.08% of the total area; the very low-value regions are the smallest. From 2012 to 2018, the areas of very low-value regions, higher-value regions, and very high-value regions decreased, while those of lower-value regions and medium-value regions expanded to a certain extent.

To verify the feasibility of the CA-Markov model in predicting the dynamic change of vegetation in the Weihe Watershed, this study took the NPP spatial distribution map of vegetation in 2006 and 2012 as basic data, simulated the NPP distribution in 2018, and performed a Kappa precision analysis with the real value to test the reliability of the model in predicting vegetation NPP. The Kappa coefficient between the 2018 NPP simulation results and the actual distribution in the Weihe Watershed was calculated as 0.8776, indicating that the simulation results achieved suitable accuracy; moreover, the simulation method and process reliability were relatively high.

Table 2. NPP area and percentage of each grade in the Weihe Watershed in 2012 and 2018

NPP Level	2012		2018	
	Area/km²	Proportion/ %	Area/km²	Proportion/ %
Very low-value regions	16,229.31	12.33	13,856.88	10.53
Lower-value regions	27,095.44	20.58	31,290.5	23.77
Medium-value regions	35,644.81	27.08	38,787.81	29.46
Higher-value regions	36,102.51	27.42	31,773.88	24.14
Very high-value regions	16,569.31	12.59	15,932.31	12.10

Based on the spatial distribution of NPP vegetation in the Weihe Watershed in 2012 and 2018, the CA-Markov model was established to predict the spatial distribution pattern

of NPP in the Weihe Watershed in 2024. Based on the spatial distribution pattern of NPP in 2018 and the predicted results of NPP in 2024, the spatial distribution pattern of NPP of the Weihe Watershed in 2030 was predicted. The predicted results for 2024 and 2030 are shown in Figure 18 and Table 3.

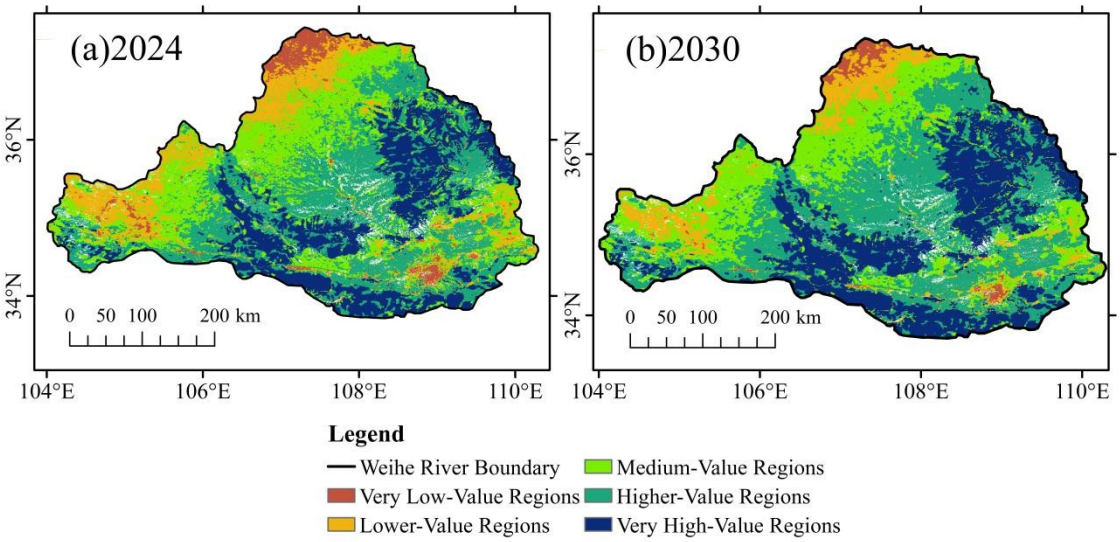

Figure 18. Spatial distribution pattern prediction of NPP in the Weihe Watershed in 2024 and 2030.

Table 3. Prediction results of NPP in the Weihe Watershed in 2024 and 2030

NPP Level	2024		2030	
	Area/km²	Proportion/%	Area/km²	Proportion/%
Very low-value regions	5,364.56	4.07	2,688.94	2.04
Lower-value regions	18,493.56	14.05	12,577.31	9.55
Medium-value regions	35,145.38	26.7	32,357.50	24.58
Higher-value regions	44,656.69	33.92	49,612.63	37.69
Very high-value regions	27,981.19	21.26	34,405.00	26.14

According to the predicted results, by 2024 the areas of very low-value regions, lower-value regions, and medium-value regions will have decreased by 6.45%, 9.72%, and 2.77%, respectively, compared to 2018. According to these results, the very low-value regions are mainly distributed north of the watershed and around Xi'an, the area of lower-value regions decreases the most and is mainly distributed in the north and west of the watershed, and the medium-value regions expand northward as a whole. The higher-value regions and very high-value regions show an expansion state, increasing by 9.79% and 9.15%, respectively, compared with 2018. The higher value regions show a trend of northward expansion, while the very high-value regions spread to the central part as a whole. By 2030, the trend will be the same. The areas of very low-value regions, lower-value regions, and medium-value regions continued to decline, decreasing by 2.03%, 4.49%, and 2.12%, respectively, compared with 2024. The areas of higher-value regions and very high-value regions continued to increase but the increase rates decrease slightly to 3.76% and 4.88%, respectively.

Overall, the prediction results of NPP dynamic changes in the Weihe Watershed indicate that in the future, the vegetation coverage will be further improved and that NPP will have a suitable development trend. Among these, the areas of very low-value regions, lower-value regions, and medium-value regions will be reduced and the overall spatial migration will be northward. The areas of higher-value regions and very high-value regions will be further increased and the spatial expansion will be northward and central.

5. Discussion

The results of this study have reference significance for the study of the vegetation growth status in the Weihe Watershed and provide a basis for the study of regional climate change and the impact and response of topography on vegetation ecosystems. Surface vegetation interacts with the atmosphere, hydrosphere, and soil sphere through material exchange and energy flow. The relationship between the degree and primary and secondary effects of many environmental factors on a vegetation system is very complex. This study focuses on analyzing several single factors of regional vegetation NPP response. However, as the influence vegetation NPP factors, such as hydrothermal conditions, physiological and ecological characteristics of the vegetation, and climate change mode of the interaction between climate factors, is relatively greater, follow-up studies will require more in-depth factors on the degree of response and vegetation NPP research, exploring more precise and reasonable analysis methods. This will help reveal the mechanisms of all kinds of environmental factors on vegetation NPP.

The spatial and temporal distribution and variation characteristics of NPP in the Weihe Watershed are closely related to human activities and economic construction, especially in the past 20 years. To develop the silk road economic belt, speeding up the urbanization process, the government introduced a series of policies and regulations, such as returning farmland to forest projects and nutrient-laden engineering. These human activities will further affect the spatial and temporal distribution and variation of vegetation NPP of the Weihe Watershed. Therefore, the influence and response of social, economic, and cultural impact factors on this subject must be further discussed in the next step. The contribution rate of various influencing factors on vegetation NPP should be evaluated, to provide effective support for further promoting ecological environment construction in the Weihe Watershed.

Finally, changes in NPP are a process complicated not only by climate change, natural disasters, and other natural factors, but also by land-use policies, social and economic development, and other human activities, as their influence on the NPP are uncertain. Therefore, setting the parameters of the CA-Markov model by considering various factors is a scientific problem to be further explored in the future.

6. Conclusions

Based on multi-source datasets, coupling the CASA model, correlation analysis, the CA-Markov model, and a variety of other methods, the NPP of the Weihe Watershed in 2000, 2006, 2012, and 2018, was analyzed and the spatial and temporal variations of the mean vegetation NPP and its response to temperature, precipitation, altitude, slope, and aspect were evaluated by reviewing the distribution and variation of vegetation NPP. Finally, the CA-Markov model was used to predict the NPP spatial distribution pattern of the Weihe Watershed in 2024 and 2030. The main conclusions are as follows:

- Concerning temporality, the seasonal and cyclical changes of NPP were obvious during the year, among which the NPP was the highest in summer and lowest in winter. In terms of specific months, NPP was the highest in July and lowest in January. The annual vegetation NPP generally showed an upward trend. Spatially, the north-south difference of the vegetation NPP is evident, showing high distribution in the south and east, and low distribution in the north and west.
- The responses of NPP to temperature and precipitation in the Weihe Watershed are significant but varied. The response to temperature is dominated by mildly positive and mildly negative correlations, which are distributed in the northern and Guanzhong Plain areas, and southern areas, respectively. The response to precipitation is a mildly positive correlation, which is distributed in the central and western regions.

Overall, the correlation between vegetation NPP and precipitation in the Weihe Watershed is higher.

- Topography has an influence on the distribution and variation of the NPP. With respect to elevation, the NPP of vegetation with increasing elevation varies greatly and shows a trend of increasing, then stabilizing, and finally decreasing. As far as the slope is concerned, the mean NPP of the vegetation increases with increasing slope. In terms of aspect, the mean NPP of the vegetation on the north and west slopes is larger, while that on the south and east slopes is smaller.
- The NPP of the Weihe Watershed will continue to improve and presents good development. The very low-value regions, lower-value regions, and medium-value regions will reduce and move north in the future. The higher-value regions and very high-value regions will increase and expand towards the northern and central regions.

Acknowledgments: The authors acknowledge the financial support granted by the "National Natural Science Foundation of China"(41471452), the Fundamental Research Funds for the Central Universities (No.300102269201, 300102299206) and the Key R & D program of Shaanxi Province(No.2020ZDLSF06-07, 2019SF-237).

Funding: This work was supported by the "National Natural Science Foundation of China"(41471452); the Fundamental Research Funds for the Central Universities (No.300102269201, 300102299206) and the Key R & D program of Shaanxi Province(No.2020ZDLSF06-07, 2019SF-237).

References

1. Guan, X.; Shen, H.; Gan, W.; Yang, G.; Wang, L.; Li, X.; Zhang, L.A. A 33-Year NPP Monitoring Study in Southwest China by the Fusion of Multi-Source Remote Sensing and Station Data. *Remote Sens.* 2017, *9* (10), 1082.

2. Zheng, Z.; Zhu, W.; Zhang, Y. Direct and Lagged Effects of Spring Phenology on Net Primary Productivity in the Alpine Grasslands on the Tibetan Plateau. *Remote Sens.* 2020, *12* (7), 1223.

3. Naeem, S.; Zhang, Y.; Tian, J.; Qamer, F.M.; Latif, A.; Paul, P.K. Quantifying the Impacts of Anthropogenic Activities and Climate Variations on Vegetation Productivity Changes in China from 1985 to 2015. *Remote Sens.* 2020, *12* (7), 1113.

4. Barnard, J.C.; Powell, D.M. A Comparison Between Modeled and Measured Clear-Sky Radiative Shortwave Fluxes in Arctic Environments, with Special Emphasis on Diffuse Radiation. *J. Geophys. Res.* 2002, *107* (D19), 9–10.

5. Bian, J.; Li, A.; Deng, W. Estimation and Analysis of Net Primary Productivity of Ruoergai Wetland in China for the Recent 10 Years Based on Remote Sensing. *Procedia Environ. Sci.* 2010, *2*, 288–301.

6. Bradford, J.B.; Hicke, J.A.; Lauenroth, W.K. The Relative Importance of Light-Use Efficiency Modifications from Environmental Conditions and Cultivation for Estimation of Large-Scale Net Primary Productivity. *Remote Sens. Environ.* 2005, *96* (2), 246–255.

7. Cao, M.; Prince, S.D.; Small, J. Remotely Sensed Interannual Variations and Trends in Terrestrial Net Primary Productivity 1981–2000. *Ecosystems* 2004, *7*, 233–244.

8. Defosse, G.E.; Bertiller, M.B. Comparison of Four Methods of Grassland Productivity Assessment Based on Festuca pallescens Phytomass Data. *J. Range Manag.* 1991, *44* (3), 199–203.

9. Field, C.B.; Randerson, J.T.; Malmström, C.M. Global Net Primary Production: Combining

Ecology and Remote Sensing. *Remote Sens. Environ.* 1995, *51* (1), 74–88.

10. Ruimy, A.; Saugier, B.; Dedieu, G. Methodology for the Estimation of Terrestrial Net Primary Production from Remotely Sensed Data. *J. Geophys. Res.* 1994, *99* (D3), 18515–18521.

11. Kalubarme, M.H.; Potdar, M.B.; Manjunath, K.R.; Mahey, R.K.; Siddhu, S.S. Growth Profile Based Crop Yield Models: A Case Study of Large Area Wheat Yield Modelling and Its Extendibility Using Atmospheric Corrected NOAA AVHRR Data. *Int. J. Remote Sens.* 2003, *24* (10), 2037–2054.

12. Lewis, J.E.; Rowland, J.; Nadeau, A. Estimating Maize Production in Kenya Using NDVI: Some Statistical Considerations. *Int. J. Remote Sens.* 1998, *19* (13), 2609–2617.

13. Jones, J.W.; Hoogenboom, G.; Porter, C.H.; Boote, K.J.; Batchelor, W.D.; Hunt, L.A.; Wilkens, P.W.; Singh, U.; Gijsman, A.J.; Ritchie, J.T. The DSSAT Cropping System Model. *Eur. J. Agron.* 2003, *18* (3–4), 235–265.

14. Prasad, A.K.; Chai, L.; Singh, R.P.; Kafatos, M. Crop Yield Estimation Model for Iowa Using Remote Sensing and Surface Parameters. *Int. J. Appl. Earth Obs. Geoinf.* 2006, *8* (1), 26–33.

15. Nemani, R.R.; Keeling, C.D.; Hashimoto, H.; Jolly, W.M.; Piper, S.C.; Tucker, C.J.; Myneni, R.B.; Running, S.W. Climate-Driven Increases in Global Terrestrial Net Primary Production from 1982 to 1999. *Science* 2003, *300* (5625), 1560–1563.

16. Doraiswamy, P.C.; Moulin, S.; Cook, P.W.; Stern, A. Crop Yield Assessment from Remote Sensing. *Photogramm. Eng. Remote Sens.* 2003, *69* (6), 665–674.

17. Zhu, W.; Pan, Y.; Zhang, J. Estimation of Net Primary Productivity of Chinese Terrestrial Vegetation Based on Remote Sensing. Chinese Journal of Plant Ecology 2007, 31 (3), 413–42.

18. Li, X.; Liang, H.; Cheng, W. Spatio-Temporal Variation in AOD and Correlation Analysis with PAR and NPP in China from 2001 to 2017. *Remote Sens.* 2020, *12* (6), 976.

19. Lai, C.; Li, J.; Wang, Z.; Wu, X.; Zeng, Z.; Chen, X.; Lian, Y.; Yu, H.; Wang, P.; Bai, X. Drought-Induced Reduction in Net Primary Productivity Across Mainland China from 1982 to 2015. *Remote Sens.* 2018, *10* (9), 1433.

20. Shang, E.; Xu, E.; Zhang, H.; Liu, F. Analysis of Spatiotemporal Dynamics of the Chinese Vegetation Net Primary Productivity from the 1960s to the 2000s. *Remote Sens.* 2018, *10* (6), 860.

21. Neumann, M.; Moreno, A.; Thurnher, C.; Mues, V.; Härkönen, S.; Mura, M.; Bouriaud, O.; Lang, M.; Cardellini, G.; Thivolle-Cazat, A.; Bronisz, K.; Merganic, J.; Alberdi, I.; Astrup, R.; Mohren, F.; Zhao, M.; Hasenauer, H. Creating a Regional MODIS Satellite-Driven Net Primary Production Dataset for European Forests. *Remote Sens.* 2016, *8* (7), 554.

22. Chen, F.; Shen, Y.; Li, Q.; Guo, Y.; Xu, L. Spatio-Temporal Variation Analysis of Ecological Systems NPP in China in Past 30 Years. *Sci. Geogr. Sin.* 2011, *31*, 1409–1414.

23. Yu, T.; Sun, R.; Xiao, Z.; Zhang, Q.; Liu, G.; Cui, T.; Wang, J. Estimation of Global Vegetation Productivity from Global LAnd Surface Satellite Data. *Remote Sens.* 2018, *10* (2), 327.

24. Neumann, M.; Zhao, M.; Kindermann, G.; Hasenauer, H. Comparing MODIS Net Primary Production Estimates with Terrestrial National Forest Inventory Data in Austria. *Remote Sens.* 2015, *7* (4), 3878–3906.

25. Wang, Y.; Xu, X.; Huang, L.; Yang, G.; Fan, L.; Wei, P.; Chen, G. An Improved CASA Model for Estimating Winter Wheat Yield from Remote Sensing Images. *Remote Sens.* 2019, *11* (9), 1088.

26. Kong, F.; Dong, Q.; Xiang, K.; Yin, Z.; Li, Y.; Liu, J. Spatiotemporal Variability of Remote Sensing Ocean Net Primary Production and Major Forcing Factors in the Tropical Eastern Indian and Western Pacific Ocean. *Remote Sens.* 2019, *11* (4), 391.

27. Zhang, M.; Lin, H.; Sun, H.; Cai, Y. Estimation of Vegetation Productivity Using a Landsat 8 Time Series in a Heavily Urbanized Area, Central China. *Remote Sens.* 2019, *11* (2), 133.

28. Luo, Z.; Wu, W.; Yu, X.; Song, Q.; Yang, J.; Wu, J.; Zhang, H. Variation of Net Primary Production and Its Correlation with Climate Change and Anthropogenic Activities over the Tibetan Plateau. *Remote Sens.* 2018, *10* (9), 1352.

29. Wang, L.; Yu, D.; Liu, Z.; Yang, Y.; Zhang, J.; Han, J.; Mao, Z. Study on NDVI Changes in Weihe Watershed Based on CA-Markov Model. *Geol. J.* 2018, *53*, 435–441.

30. Dungan, J. Spatial Prediction of Vegetation Quantities Using Ground and Image Data. *Int. J. Remote Sens.* 1998, *19* (2), 267–285.

31. Ji, L.; Peters, A.J. Forecasting Vegetation Greenness with Satellite and Climate Data. *IEEE Geosci. Remote Sensing Lett.* 2004, *1* (1), 3–6.

32. Iwasaki, H. NDVI Prediction over Mongolian Grassland Using GSMaP Precipitation Data and JRA-25/JCDAS Temperature Data. *Journal of Arid Environments* 2009, *73* (4–5), 557–562.

33. Fernández-Manso, A.; Quintano, C.; Fernández-Manso, O. Forecast of NDVI in Coniferous Areas Using Temporal Arima Analysis and Climatic Data at a Regional Scale. *Int. J. Remote Sens.* 2011, *32* (6), 1595–1617.

34. Funk, C.C.; Brown, M.E. Inter-Seasonal NDVI Change Projections in Semi-Arid Africa. *Remote Sens. Environ.* 2006, *101*, 549–256.

35. Gonçalves, R.R.V.;Jr; Zullo, J.; Romani, L.A.S.; Nascimento, C.R.; Traina, A.J.M. Analysis of NDVI Time Series Using Cross-Correlation and Forecasting Methods for Monitoring Sugarcane Fields in Brazil. *Int. J. Remote Sens.* 2012, *33* (15), 4653–4672.

36. Wang, L.; Yu, D.; Liu, Z.; Zhang, S.; Yang, Y. Study on Tempo-Spatial Variations of NDVI and Climatic Factors and Their Correlation in the Weihe Watershed. *Res. O.D. Soil Water Conserv.* 2019, *26*, 249–254.

37. Li, H.; Bai, Y.; Yang, S.; Zhu, X.; Zhao, K. Prediction of Vegetation Dynamic Changes in Central Nujiang Watershed Based on Markov Process Model. *Chin. J. Ecol.* 2009, *28*, 371–376.

38. Zhang, M.; Huang, C.; Mi, N.; Wang, X.; Qu, H. Combination Forecast Model of NDVI Based on Support Vector Machine Regression. *J. Hebei Univ. Technol.* 2017, *46*, 39–45.

39. Zhang, R.; Zhang, X. The Evolution of the Ecological Environment in Shaanxi Part of Weihe River Basin in Recent 50 Years. *J. Arid Land Resour. Environ.* 2008, *22*, 37–42.

40. Wang, L.; Zhang, M.; Sui, L.; Zhang, S.; Yang, Y. Ecological Function Regionalization in the Weihe River Basin. *Arid Zone Res.* 2020, *37*, 236–243.

41. Potter, C.S.; Randerson, J.T.; Field, C.B.; Matson, P.A.; Vitousek, P.M.; Mooney, H.A.; Klooster, S.A. Terrestrial Ecosystem Production: A Process Model Based on Global Satellite and Surface Data. *Global Biogeochem. Cycles* 1993, *7* (4), 811–841.

42. Field, C.B.; Behrenfeld, M.J.; Randerson, J.T.; Falkowski, P. Primary Production of the Biosphere: Integrating Terrestrial and Oceanic Components. *Science* 1998, *281* (5374), 237–240.

43. Zhu, W.; Pan, Y.; Liu, X.; Wang, A. Spatio-Temporal Distribution of Net Primary Productivity Along the Northeast China Transect and Its Response to Climatic Change. *J. of For. Res.* 2006, *17* (2), 93–98.

44. Zhu, W.; Chen, Y.; Pan, Y.; Li, J. Estimation of Light Utilization Efficiency of Vegetation in China Based on GIS and RS. *Geom. Inf. Sci. Wuhan Univ.* 2004, *29*, 694–698.

45. Zhu, W.; Chen, Y.; Xu, D.; Li, J. Advances in Terrestrial Net Primary Estimation Models. *Chin. J. Ecol.* 2005, *24*, 296–300.

46. Karimi, H.; Jafarnezhad, J.; Khaledi, J. Monitoring and Prediction of Land Use/Land Cover Changes Using CA-Markov Model: A Case Study of Ravansar County in Iran. *Arab. J. Geosci.* 2018, *11*, 1–9.

47. Chuang, C.; Lin, C.; Chien, C.; Chou, W. Application of Markov-Chain Model for Vegetation Restoration Assessment at Landslide Areas Caused by a Catastrophic Earthquake in Central Taiwan. *Ecol. Modell.* 2011, *222* (3), 835–845.

48. Durmusoglu, Z.O.; Tanriover, A.A. Modelling Land Use/Cover Change in Lake Mogan and Surroundings Using CA-Markov Chain Analysis. *J. Environ. Biol.* 2017, *38* (5(SI)), 981–989.

49. Gong, Z.; Cui, T.; Pu, R.; Lin, C.; Chen, Y. Dynamic Simulation of Vegetation Abundance in a Reservoir Riparian Zone Using a Sub-Pixel Markov Model. *Int. J. Appl. Earth Obs. Geoinf.* 2015, *35*, 175–186.

50. Yu, Y.; Wang, Y.; Qin, F.; Guo, P. Vegetation Index Change and Its Response to Climate in Henan Province. *J. For. Environ.* 2019, *39*, 280–286.